

B+ANN: A Fast Billion-Scale Disk-based Nearest-Neighbor Index

Selim Furkan Tekin*
 Georgia Institute of Technology
 Atlanta, Georgia
 stekin6@gatech.edu

Rajesh Bordawekar
 IBM T. J. Watson Research Center
 Yorktown Heights, New York
 bordaw@us.ibm.com

ABSTRACT

Storing and processing of embedding vectors by specialized Vector databases (VDBs) has become the lynchpin in building modern AI pipelines. Most current VDBs employ variants of a graph-based approximate nearest-neighbor (ANN) index algorithm, HNSW, to answer semantic queries over stored vectors. Inspite of its wide-spread use, the HNSW algorithm suffers from several issues: in-memory design and implementation, random memory accesses leading to degradation in cache behavior, limited acceleration scope due to fine-grained pairwise computations, and support of only semantic similarity queries. In this paper, we present a novel disk-based ANN index, B+ANN, to address these issues: it first partitions input data into blocks containing semantically similar items, then builds an B+ tree variant to store blocks both in-memory and on disks, and finally, enables hybrid edge- and block-based in-memory traversals. As demonstrated by our experimental evaluation, the proposed B+ANN disk-based index improves both quality (Recall value), and execution performance (Queries per second/QPS) over HNSW, by improving spatial and temporal locality for semantic operations, reducing cache misses (19.23% relative gain), and decreasing the memory consumption and disk-based build time by 24x over the DiskANN algorithm. Finally, it enables dissimilarity queries, which are not supported by similarity-oriented ANN indices.

PVLDB Reference Format:

Selim Furkan Tekin* and Rajesh Bordawekar. B+ANN: A Fast Billion-Scale Disk-based Nearest-Neighbor Index. PVLDB, 14(1): XXX-XXX, 2020.
 doi:XX.XX/XXX.XX

PVLDB Artifact Availability:

The source code, data, and/or other artifacts have been made available at URL_TO_YOUR_ARTIFACTS.

1 INTRODUCTION

With the rise of deep learning architectures, pioneered by the natural language processing (NLP) models, latent information from unstructured [41, 53] and structured data [9, 10] can now be encoded into high-dimensional vector representations known as *embeddings*. The semantic relationships among such diverse types of data can then be quantitatively captured via distance metrics (e.g., euclidean or cosine similarity) computed over their embeddings.

This work is licensed under the Creative Commons BY-NC-ND 4.0 International License. Visit <https://creativecommons.org/licenses/by-nc-nd/4.0/> to view a copy of this license. For any use beyond those covered by this license, obtain permission by emailing info@vlbd.org. Copyright is held by the owner/author(s). Publication rights licensed to the VLDB Endowment.

Proceedings of the VLDB Endowment, Vol. 14, No. 1 ISSN 2150-8097.
 doi:XX.XX/XXX.XX

Method	On Disk	Hybrid-Mem. Search	Dissimilarity S.	Memory Cap	View Creation	Async. Update	Arch. Agnostic
HNSW [38]	✗	✗	✗	✗	✗	✗	✓
DISKANN [30]	✓	✗	✗	✗	✗	✗	✗
SPTAG [13]	✓	✗	✗	✗	✗	✗	✗
SCANN [24]	✗	✗	✗	✗	✗	✗	✗
B+ANN	✓	✓	✓	✓	✓	✓	✓

Table 1: Functionality Comparison of widely used ANN algorithms and B+ANN.

This has revolutionized the storage and processing of information and triggered the emergence of a new class of data management systems, termed as Vector databases (VDBs). VDBs are being widely adopted for storing and processing semantic vector embedding representations of large-scale structured and unstructured content[15, 19, 27, 28, 46, 54, 57]. The interest in exploiting VDBs grew enormously with the collaboration of VDBs and Large Language Model (LLM) pipelines, such as those built around models like OpenAI GPT, Google Gemini, Anthropic Claude, and others. These pipelines generate responses with the retrieved context gathered by the similarity search in the VDBs, which is known as Retrieval Augmented Generation (RAG) [36]. The wide-spread use of VDBs has motivated researchers to revisit the core technical feature of VDBs: *similarity search* index algorithms. Essentially, given a similarity query, each VDB retrieves the top- k nearest embeddings for that query using an index. Since calculating the exact Nearest Neighbors (NN) takes $O(N^2)$ complexity, approximate nearest neighbor (ANN) indexing algorithms are used to decrease the search time up to $O(\log N)$ at the cost of accuracy. The speed of algorithms depends on two factors: (i) the number of distance computations to reach the final answer, and (ii) the number of memory and disk retrievals performed before reaching a sufficiently similar vector to the query in the database. Even though there is a tremendous amount of activity for targeting the first factor, most algorithms assume the data will be stored in memory and disregard factor (ii) and the locality of stored data.

Combined with the proliferation of unstructured data and the growing interest in creating semantic relations in real-time, applications require VDBs that can store petabytes of data and run similarity search algorithms within seconds. Therefore, the assumption of adequate memory for searching is untenable, rendering in-memory algorithms impractical. Recent works such as [13, 14, 30, 50] have proposed disk-based solutions that leverage SSDs and `mmap()` system calls. They adopt graph-based solutions inspired by the Hierarchical Navigable Small Worlds (HNSW) [38], which is the most popular ANN indexing algorithm. However, as demonstrated in this paper, HNSW, an *in-memory* ANN index, performs numerous random memory accesses, resulting in a high rate of cache misses, and

*This work was done while the author was at IBM T. J. Watson Research Center.

at every step, performs small numerical computations that are difficult to optimize. Transitioning to the disk-based implementation exacerbates the problem as these algorithms rely on `mmap()`-based access without optimizing for memory locality. Furthermore, persisting the constructed index to disk while maintaining high spatial locality is particularly challenging for complex data structures such as graphs, where each node must additionally store multiple edge connections.

Alongside these, the VDBs are an emergent technology that lacks most of the capabilities and system-based optimizations of traditional relational databases. Most notably, while the temporal characteristics of subsequent queries is exploited in relational databases, VDBs are still considered as a one-shot query matching mechanism without temporal correlation. However, in a conversation with a chatbot in a RAG system, users can ask temporally related questions as shown in Figure 2b. Considering the growth of agentic systems and the pursuit of researchers to decrease time to first token (TTFT) and inter-token latency (ITL), there is a high need for a mechanism that exploits the temporal correlation for an interactive experience with the user. In relational databases, it is possible to make fine-grained access with designed access control patterns by a buffer mechanism that maximize the cache coherency; in contrast, VDBs provide only coarse-grained or no access control mechanisms. Moreover, the modern relational database systems contains many functionalities such as filtering and join operations not only for similarity but also for dissimilar queries (e.g., Db2 z/OS SQL Data Insights AI_SIMILARITY and AI_COMMONALITY queries [28]), whereas, most VDBs only provide most similar vectors for a given query. The dissimilarity task is not easily achievable, due to current indexing algorithms are based on graphs connecting vertices with their most-similar nearest neighbor. Therefore, a dissimilar query usually oscillates between two furthest vertices in the graph that are highly unrelated.

To this end, this paper targets a similarity search indexing algorithm for VDBs that incorporates memory control, buffering, paging, persistence management, cache efficiency, and the leveraging of temporal correlations. We propose B+ANN, a billion-scale, disk-based, and memory-efficient ANN indexing algorithm. As the first line of attack on the indexing problem, we recursively partition the subspace by hierarchical clustering to obtain many clusters and their centroids. Then, we repurpose the widely used B+ Tree approach to the vector domain via using the centroids as keys and vectors as values. Our generated B+ANN tree has low complexity and can be stored on the disk by maximising locality between semantic vectors, and provides a fine-grained access control mechanism during traversal. Second, we create skip-connections between leaves of the in-memory version of the B+ANN tree to perform graph traversal for the most precise searches. The resulting tree index converges in fewer hops, is more precise, faster, and easier to parallelize by exploiting local data storage and improved memory locality. The B+ANN algorithm coalesces the batched queries to increase compute granularity, while graph-based approaches of VDBs perform pair-wise the distance computations that are too fine-grained to be accelerated efficiently. Third, we introduce *semantic views* that can be extracted from the tree to represent subsets of information that create a context for a given query. Subsequent queries are answered from the query-specific view, which allows

contextualized searches that are optimized for related semantic queries. We show that the view can survive for up to a thousand queries if they are given temporally correlated.

Table 1 compares and summarizes key features of the B+ANN ANN index against a set of widely used indexing algorithms. We now highlight key contributions from our work:

- The B+ANN is designed from ground-up to be a disk-based ANN index. The choice of a B+ tree inspired data structure, allows the index to use the same data structure for both disk-based and in-memory processing.
- The in-memory B+ANN tree enables *hybrid* traversals over the tree nodes either using *skip* edges to access individual nodes or via edges between individual vectors across tree nodes.
- By exploiting semantic relationships, we improve spatial locality by storing the semantically-close vectors in physically-close disk and in-memory locations. We demonstrate that our design improves both quality and search performance while decreasing cache misses up to 19.23% relative gain and the index built time by 24x.
- Once the locality of the ANN index is improved, the overall search problem becomes compute-bound. Moreover, small pairwise compute vector operations can be now batched into coarse-grained matrix computations and can be accelerated using hardware accelerators such as SIMD and GPUs.
- We leverage our spatial-locality optimized design to enable faster response time and longer view survival time of the temporally correlated queries, such as those generated in Agentic scenarios.
- Our design incorporates unique functionalities of recent AI-enabled relational databases (e.g., supporting dissimilarity queries) that are largely unexplored in VDBs.

The remainder of this paper is organized as follows. Section 2 reviews the related work and highlights the key differences between our approach and existing methods. Section 3 presents the preliminaries and fundamental concepts necessary to understand the proposed framework. Section 4 formalizes the problem setting and defines the main objectives. Section 5 details our proposed methodology and system design. Section 6 reports the experimental evaluation and performance analysis. Finally, Section 7 concludes the paper with summarizing remarks and discussions on potential future directions.

2 RELATED WORK

Similarity search algorithms have been studied for half century and more [47]. Today, in the rise of AI, they have become the cornerstones of the vector databases [26] such as Milvus [54], Elasticsearch [19], Analytics-DB [57], ChromaDB [15], and PASE [57]. The popularity of the vector databases has grown significantly due to the use of Maximum Inner Product Search (MIPS) to retrieve necessary context for a query to a LLM, which is known as Retrieval Augmented Generation (RAG) [36]. Due to their referencing property, vector databases are becoming increasingly prevalent systems alongside LLMs. This has also led to the development of hybrid queries containing attribute predicates such as giving a date range together with *top-k* searches [22, 59].

There have been numerous approaches to ANNs in the literature mainly focus on the high-recall search with high throughput and

low latency. The approaches follow two main ideas: First, partitioning the vector space into many sub-spaces to reduce the search space iteratively, and second, creating proximity-based graphs and navigating the closest node based on the query. In the partition-based approaches, the space is divided by following clustering, hash, or tree based solutions.

Representative clustering based solutions, such as, [7, 8] utilize inverted indices (IVF) by dividing the space with clustering algorithms such as K-means, and assigning a centroid as an index to represent all the vectors in the subspace. The quantization based approaches, such as Product Quantization (PQ) [33] further divide the input queries and the vectors by slicing into M subspaces and encoding them into codes to reduce the cost of storage [31, 55]. Two consecutive works [24, 52] further improved the quantization performance by dynamic weighting on the reconstruction loss based on the query. Johnson et al. [32] employ both PQ and IVF, called as IVFPQ, to index billion scale data. However, IVF can cause imbalanced partition on the data where some subspaces can be overly populated.

The hash-based solutions such as locality sensitive hashing (LSH) [3, 4, 11, 17, 34], maps the close vectors into the same buckets and reach the candidate vectors that fall into the same bucket with the query. The algorithm works in sub-linear time and have theoretical guarantees on the query accuracy [29, 56]. However, the hash table can grow significantly and they are outperformed by more recent graph-based approaches.

The tree-based solutions follow classical data structures to index the vectors such as KD-Tree [20], R-Tree[25], and M-Tree [16], however, their performance are limited with the number of dimensions. For example, the KD-tree needs to alternate in every dimension to find the closest leaf by traversing one-dimension at a time. Thus, Muja and Lowe [42] proposed high-dimensional tree-based solution by creating an hierarchical tree with the recursive K-means clustering. The constructed tree searches the query based on priority queue sorted by distance to the next level nodes. Similarly, Spotify [51] proposed hierarchical tree constructed by dividing the space with hyperplanes passing between two randomly selected points in each recursive call. However, in both methods, the resulted trees can be very deep and unbalanced, in addition, the insertions to the trees are ignored.

Instead of partitioning the space, the graph-based solutions, such as HNSW, start with an empty graph and add each vector as a vertex. The vertices are connected based on the distances to other vertices [38]. The connectivity of the graph is an hyper parameter where high connectivity creates less error but high latency. To increase the search speed and escape from dense hubs, the constructed graphs can contain skip connections [39] or shortcuts across different levels of HNSW graph [23]. MARGO [58] proposes a monotonic path-aware graph layout on disks. Recently, more hybrid approaches such as [30, 43] are introduced by utilizing hierarchical clustering and creating a graph in each partition with strict connectivity. Then, the created graphs are merged to create one final graph with strong connectivity with a larger search space. These methods also utilize in-search updates to perform pruning on the edges. However, these updates cause per-vertex locks in parallel setup. The most recent approach [40] proposed a better scaling parallelization of these algorithms with the generous assumption of memory ($> 1\text{TB}$). In

addition to high memory cost, they start from random seed node in each search operation resulting lots of cache misses with random memory accesses.

Recent works focusing on disk utilization (SSDs) and being able to scale in billion with more modest memory assumption (64 – 128GB) include DiskANN [30], HM-ANN [49], and SPANN [14]. DiskANN stores the large data such as full-precision vectors and the graph on the SSD, while it uses the compressed vectors during search time to traverse on the graph. However, the final ranking of the candidate vectors uses the full-precision vectors, and it also suffers from the latency caused by the random disk accesses. HM-ANN divides the memory into two by placing pivot points in fast and NSW graphs in to slow memory. Still, it ends-up causing 1.5 times more fast memory consumption. Lastly, SPANN stores the uncompressed posting lists in disk (SSDs) and centroids in memory. It partitions the space by following an hierarchical balanced clustering. However, the hierarchy of the created tree is not fully utilized, i.e. only the leaf nodes are used. The algorithm also requires multiple in-search update steps to keep the tree balanced.

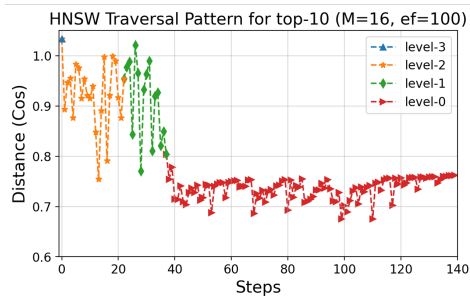
Furthermore, utilization of GPUs into the ANN distance calculations prevail among more recent systems such as FAISS [18], SONG [60] and CAGRA [45] (available in the Nvidia cuVS [44] library). Compared to FAISS, SONG and CAGRA accelerate graph-based ANN on Nvidia GPUs, by exploiting advanced Nvidia CUDA features such as the *warp* functions.

3 PRELIMINARIES

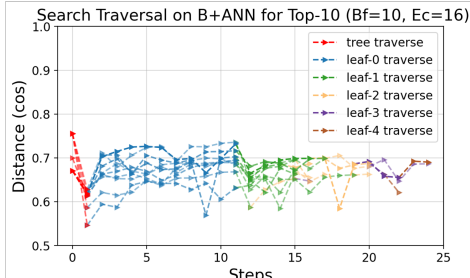
3.1 Random Accesses of HNSW

The growing popularity of vector databases leads to increased utilization of ANN algorithms, which enable fast similarity search while balancing accuracy and computational efficiency. HNSW, in this matter, is ubiquitous for the most popular VDBs, e.g., Chroma, Milvus, and pgVector, which is an open-source PostGRES extension that supports vector data types and enables ANN search, including HNSW. The reasons for the widespread use of HNSW are that it offers flexibility and performance with efficient updates, without degradation in recall performance. However, as we demonstrate in this section, HNSW is not cache-efficient, as it employs a greedy-based traversal with random initiations, resulting in cache misses and slower memory accesses that exacerbate in disk-resident executions.

Figure 1a presents an empirical proof of these problems. HNSW starts at a random location at the highest layer and traverses to the lower layers by jumping between the nodes until it reaches the closest vicinity of the query vector it can find. First, every visit to a node is an access to the memory, where the nodes are located randomly in memory. Second, in each visit, the greedy search calculates the distance between the query and the node’s edges in a fine-grained manner through pairwise distance computation. As an alternative, we propose a more efficient solution to these two aspects by a *hybrid* design of combining the B+Tree structure with the modified greedy-search between leaf nodes, similar to HNSW. B+ANN preserves node locality by placing semantically related vectors in close physical proximity within memory or disk, and further improves cache coherence. Second, as illustrated in Figure 1b, a leaf-node in the B+ANN contains multiple vectors, which allows batch loading



(a)



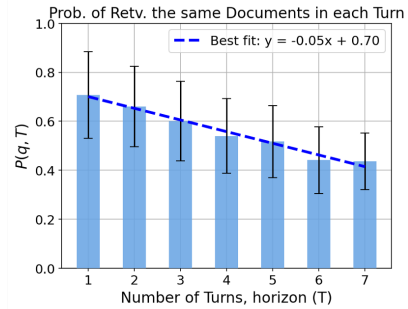
(b)

Figure 1: (a) The figure illustrates the HNSW retrieval pattern from the highest to the lowest level. Each visit to a node involves accessing memory and performing a pairwise distance calculation. (b) The retrieving pattern of B+ANN. The first phase is the tree traverse, and the second phase is the skip-edge connections. Each leaf node incurs one memory access, followed by a vector–matrix operation that computes the distances between the query and all vectors stored in the leaf. Note that the number of B+ANN steps (23) is substantially lower than HNSW (140).

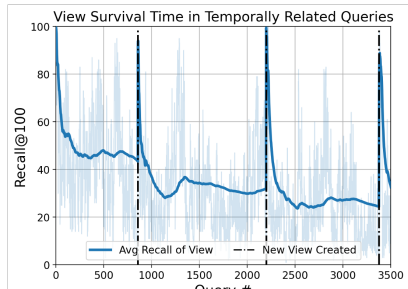
and faster distance calculation operations over multiple vectors, e.g., using matrix multiplication instead of pair-wise dot-products. Therefore, with one I/O operation, we can load many close vectors to the query and calculate distances for more vectors at a time, and during the traversal, the next leaf location is in proximity, thereby reducing access time.

3.2 The Temporal Correlation in Retrievals

Consider a Retrieval Augmented Generation (RAG) system and user interaction in a multi-turn conversation. It is highly probable that the first question asked by the user will be related to the following questions. On this basis, it is also expected that the retrieved information from a database for questions will overlap and intersect. Therefore, there is a temporal relation between the vectors retrieved in each turn of conversation. The left plot in Figure 2a shows an experiment on a multi-turn conversation dataset of a RAG system, MTRAG [35], providing experimental evidence. As the number of turns increases, the probability of retrieving the same documents decreases from 0.7 to 0.4, showing that there is a high temporal relationship between consecutive queries. In light of this observation, we design a modified B+Tree structure and introduce the



(a)



(b)

Figure 2: (a) We show our observation in multi-turn conversation of a RAG system [35]: The probability of retrieving the same document in a conversation with an LLM for each turn. (b) Our proposed view creation system which exploits the temporal relation of successive queries.

create_view function that puts a granular perspective of a subset of the database into the memory and responds in-memory (see Section /refsec:buildtree for more details). The right plot on Figure 2b shows how long a view can respond to temporally correlated queries until the asked query is not found in the view. The spikes show that the recall of the queries are highest once the view is created, and it degrades as more queries come.

A key functionality of a B+Tree structure is the sequential access support by traversing the leaf nodes for range queries. In our modified B+Tree structure, where the keys are centroids of clusters and values are the vectors stored in those clusters, we created *skip connections* between leaf nodes (see Section 5.3 for more details). If the incoming queries are temporally correlated, the subsequent vectors are likely to reside in the same node or in neighboring nodes. By traversing adjacent leaf nodes, these vectors can be retrieved with improved memory access efficiency and cache locality. Therefore, B+ANN excels at temporally correlated queries by mapping temporal relations to the spatial localities of vectors. B+ANN is not limited with these functionalities as shown in Table 1. In the following sections, we talk about methodology and other features of our design. We begin by describing the ANN problem and defining our essential elements at our formulation.

4 PROBLEM FORMULATION

For a vector collection $\mathcal{D} = \{\mathbf{x}_i\}_{i=0}^N$ of N vectors, where each $\mathbf{x}_i \in \mathbb{R}^n$ represents the extracted semantic information, e.g., embedding, of a sample in the database with dimensionality of n . A distance function $d : \mathbb{R}^n \times \mathbb{R}^n \rightarrow \mathbb{R}$ maps vectors $\mathbf{x}_i, \mathbf{x}_j$, where $i, j = 1, \dots, N$ onto a scalar distance $d(\mathbf{x}_i, \mathbf{x}_j) = s$. Multiple distance functions can be used, e.g., Hamming, Minkowski, Mahalanobis but most commonly Euclidean distance (L_2 norm), and cosine distance ($1 - \cos(\theta)$) are used. Larger distances indicate more dissimilar input vectors, and zero indicates identical vectors. For the search of the most similar vectors, we define the following elements:

Definition-1: (*k*-Nearest Neighbors) (*k*-NNs) Given a vector collection \mathcal{D} and a query \mathbf{q} in the same Euclidean space \mathbb{R}^n , NN aims to find k nearest neighbors \mathcal{R} of \mathbf{q} by calculating a distance $d(\mathbf{x}, \mathbf{q})$ for each $\mathbf{x} \in \mathcal{R}$, i.e.,

$$R(\mathbf{q}, k) = \underset{\mathcal{R} \subset \mathcal{D}, |\mathcal{R}|=k}{\operatorname{argmin}} \sum_{\mathbf{x} \in \mathcal{R}} d(\mathbf{x}, \mathbf{q}). \quad (1)$$

Here $R : Q \rightrightarrows \binom{\mathcal{D}}{k}$ is the set-valued map from query set Q to the set of k -subsets of \mathcal{D} . The time complexity of the brute-force k -NN algorithm is $O(k \cdot N \cdot n)$. For large vector collections ($|\mathcal{D}| \gg$ billions), brute-force NNs are highly impractical. Therefore, researchers relaxed the definition of NNs and introduced *Approximate Nearest Neighbor* (ANNS) algorithms, allowing more practical implementations with efficiency-accuracy trade-offs.

Definition-2: (*k*-ANN) ANNS builds an index \mathcal{I} over the dataset \mathcal{D} , which maps the input query $\mathbf{q} \in \mathbb{R}^n$ to a subset $C \subseteq \mathcal{D}$. At each step of propagation on the \mathcal{I} , it computes distances $d(\mathbf{x}, \mathbf{q})$ between query and vectors $\mathbf{x} \in C$ to obtain the approximate k nearest neighbors $\tilde{\mathcal{R}}$ of \mathbf{q} . The result is sufficiently close to the true set \mathcal{R} with the gain in efficiency. To measure the level of correctness, recall at a subset size defined as follows:

Definition-3: (*Recall-k@k'*) Let $\tilde{\mathcal{R}} \subset \mathcal{D}$ be the output of ANN index \mathcal{I} with size k' for a query \mathbf{q} and \mathcal{R} be the true k -NNs of \mathbf{q} . Then the *Recall-k@k'* of \mathbf{q} is $\frac{|\tilde{\mathcal{R}} \cap \mathcal{R}|}{|\mathcal{R}|}$. The most common choice of recall is 10@10, yet recently, in RAG systems, it is more common to use broad-retrieval and perform re-ranking among the retrieved top-100 vectors using re-ranking models [2, 12, 21]. In this paper, therefore, we focused on the recall 10@10 and 100@100.

The index of B+ANN, \mathcal{I} , is a combination of Tree-based and Graph-based indexing due to the skip-edge connections. The Tree-based structure partitions \mathcal{D} by making a small number of comparisons while still reaching sufficiently close vectors to the input query \mathbf{q} . Then, the Graph-Based structure, created by skip-connections, follows edges that lead to closer points in the graph with varying hop sizes. Based on these, we define the Tree and Graph indexing as follows:

Definition-4: (*Tree-based Indexing*) Given a finite dataset \mathcal{D} in \mathbb{R}^n , a rooted tree denoted by $\mathcal{T} = (\mathcal{V}, \mathcal{E}, r)$ constructed on \mathcal{D} as index $\mathcal{T}(\mathbf{q}, k)$ that returns k -ANNs. It consists of a set of vertices \mathcal{V} , a set of directed edges $\mathcal{E} \subseteq \mathcal{V} \times \mathcal{V}$, and a root node $r \in \mathcal{V}$. For any vertex, there is only one vertex that is connected to it, $\forall v \in \mathcal{V} \setminus \{r\}$, we have $\exists! u \in \mathcal{V}, (v, u) \in \mathcal{E}$. To represent the hierarchy, each branch of the tree can be thought of as a subtree; then we can also define $\mathcal{T} = \{r, [\mathcal{T}_1, \mathcal{T}_2, \dots, \mathcal{T}_k]\}$ for a rooted tree with k branches. We define the parent-child relation as $\operatorname{parent}(v) = u$ if $(u, v) \in \mathcal{E}$

and $\operatorname{children}(v) = \{u \mid (v, u) \in \mathcal{E}\}$. Therefore, the set of leaf nodes of \mathcal{T} is denoted as $\mathcal{L}(\mathcal{T}) = \{v \in \mathcal{V} \mid \operatorname{children}(v) = \emptyset\}$. Tree-based ANN reaches the $\tilde{\mathcal{R}}$ by traversing from the root toward the leaves, selecting at each step the branch whose subspace (or cluster) is closest to the query. Each selected branch represents a hierarchical partition of the data space where the children of the selected parent reside. Once the lowest level (leaves) is reached, the search terminates by returning the top- k closest vertices.

Definition-5: (*Graph-based Indexing*) Given a dataset \mathcal{D} , a graph denoted by $G = (\mathcal{V}, \mathcal{E})$ is constructed as index $G(\mathbf{q}, k)$ that returns k -ANNs. Here, \mathcal{V} is the set of vertices denoted by $v, u \in \mathcal{V}$ and have neighborhood relationship $(u, v) \in \mathcal{E}$. For a query \mathbf{q} , seeds $\tilde{\mathcal{C}}$, routing strategy, and terminal condition, G conducts search starting from $\tilde{\mathcal{C}}$ and continuously find subsets $C \subseteq \mathcal{D}$ via routing strategy until C satisfies the terminal condition. The algorithm returns nearest vectors in C as approximate k -NNs $\tilde{\mathcal{R}}$.

Definition-6: (*View*) For a given dataset \mathcal{D} , the tree-based index \mathcal{T} , a query q_t at time t , and size of view k , a view is extracted from the \mathcal{T} by k -ANNs of \mathbf{q} to create a sub-tree \mathcal{T}' , which is denoted as follows:

$$\begin{aligned} V(q_t, \mathcal{T}, k) &= \mathcal{T}', \\ \text{s.t. } \mathcal{T}' &= (\mathcal{V}', \mathcal{E}', r'), v \in \mathcal{T}(q_t, k) \text{ and } v \in \mathcal{V}' \end{aligned} \quad (2)$$

where, V denotes the view function that constructs a single tree \mathcal{T}' from the set of k -ANNs of the query \mathbf{q} , retrieved by the base index $\mathcal{T}(q_t, k)$. Consequently, \mathcal{T}' represents a local tree structure induced by the k retrieved vectors that approximate the neighborhood of \mathbf{q} . For the upcoming queries $q_{>t}$, the sub-tree \mathcal{T}' index and returns the k -ANNs.

Building on these definitions, next, we show our methodology to build B+ANN, how it indexes the queries, and unique functionalities to make optimum accesses with the least memory footprint.

5 METHODOLOGY

Based on the motivations presented in Section 3, Figure 3 illustrates the three phases of our design, B+ANN indexing. In this section, we cover the details of each phase, building upon the definitions provided in Section 4.

5.1 Recursively Partitioning by Hierarchical Clustering

Considering the data of a large dataset ($|\mathcal{D}| \gg$ billions) covering the space, it is common to observe non-uniform data distributions forming local hubs with thousands of vectors close to each other. When partitioning the space into subregions, the partitioning scheme should be adaptive to this distribution, allocating finer partitions to dense regions to better capture their local structure. To tackle the imbalanced partitioning, we perform recursive K-Means clustering. Specifically, we use K-means++ Clustering [5], which reduces number of iteration compared to standard K-means and it finds better initial centroids by initializing them furthest to every other centroid. The algorithm is shown in Algorithm 1 which takes four parameters: dataset \mathcal{D} , number of clusters in each K-Means operation K , the threshold value τ , which is the maximum number of vectors exists in a cluster, and J is the number of expectations-maximization steps that each K-Means run.

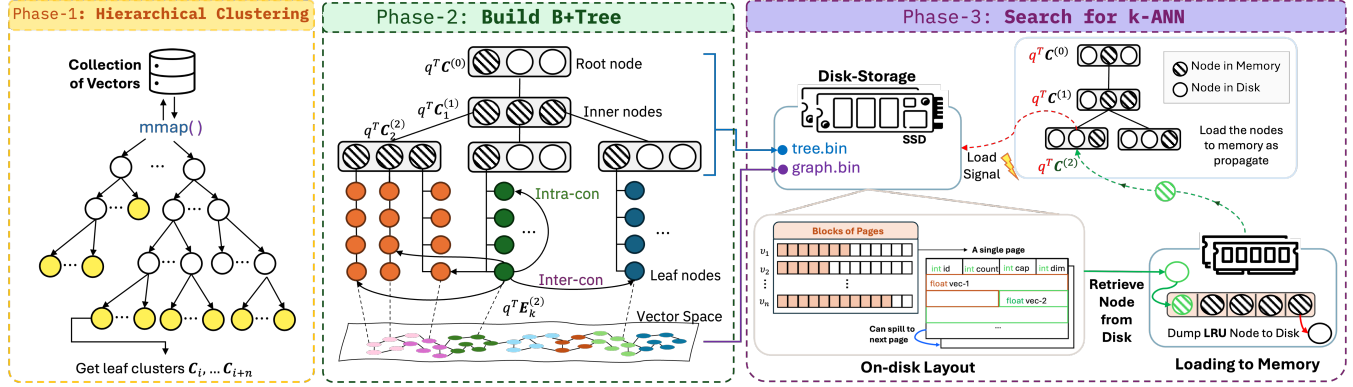


Figure 3: We show the three phases of B+ANN Indexing. First phase partitions the vector space with hierarchical clustering. The second phase builds the B+ANN tree with skip-edge connections. The third phase indexes the query and performs accesses.

Algorithm 1 Hierarchical Clustering

```

1: procedure HCLUSTER( $\mathcal{D}$ ,  $\tau$ ,  $K$ ,  $J$ )
2:    $q = \text{Queue}()$ , clusters = [ ]
3:    $q.\text{push}(\mathcal{D})$                                  $\triangleright$  Add the initial data to the queue
4:   while  $!q.\text{empty}()$  do
5:     data_part  $\leftarrow q.\text{pop}()$ 
6:     clustered_data  $\leftarrow \text{Kmeans}++(\text{data\_part}, K, J)$ 
7:     for  $i = 1$  to  $K$  do
8:       if clustered_data[ $i$ ].size()  $> \tau$  then
9:         clusters.add(data_part)
10:      else
11:         $q.\text{push}(\text{clustered\_data}[i])$ 
12:      end if
13:    end for
14:   end while
15:   return clusters                                 $\triangleright$  Return Clusters
16: end procedure

```

As shown in line 8, the algorithm adds the partitioned data into the queue since it has a size higher than the threshold τ . The popped stack contains the next data to be partitioned into clusters, as shown in line 6. Each clustering operation on a data partition creates another level at the hierarchical tree, as shown in Phase-1 in Figure 3. Where the leaves contains the final clusters C_1, \dots, C_m with cluster count m and each cluster having less than τ vectors denoted by $C_i = [\mathbf{x}_{i,1}, \dots, \mathbf{x}_{i,n'}]$, where $n' \leq \tau$ and $\mathbf{x}_{i,j} \in \mathcal{D}$.

Considering the computational cost, a K-means clustering operation has $O(K \times N \times J)$ complexity without considering the dimensionality of the vectors. The height of hierarchical tree is $\log_K(N)$, thereby, total Hierarchical Clustering has complexity of $O(K \times N \times J \times \log_K(N))$. Another crucial point is the memory cost, as line 3 indicates, when the first K-Means++ algorithm is applied on the full dataset, the cost can drastically increase. Loading the dataset at once into the memory can cause an OOM error and is dangerous; therefore, we employ `mmap()` system-call to let the OS handle the memory management during the Hierarchical Clustering. The vectors remain accessed through their memory-mapped

representation until the tree construction is completed. Lastly, during the creation of clusters, we keep track of the hierarchy to use in our B+ Tree-inspired index creation.

5.2 Building and Indexing B+ANN Tree

B+ Tree is prominent for single-column indexing in relational databases, and due to its flexibility, it grows wide with low height, resulting in $O(\log N)$ complexity for search/insert/delete operations and $O(N \log N)$ complexity to build. The data is stored in leaves, and the inner nodes are only used for navigation. This allows better control of the memory by storing the inner nodes in memory and leaves in disk. With a buffer system that loads leaves from disk to memory from a block-oriented storage, it allows fine-grained control over the data for memory management. A differentiating factor of the B+Tree indexing is its sequential and range query performance, since the data is stored in leaves, and it can traverse from one link to another without going to the higher layers. Overall, a significant amount of experience and development has been made in relational vector databases and particularly in B+Tree algorithms. As the motivations of vector and relational databases are analogous, thereby, we adapt the B+ Tree indexing to vectors by using cluster centroids $\mathbf{c}_i^{(l)}$ as keys and their vectors \mathbf{v}_j as values. Here, a centroid is defined:

$$\mathbf{c}_i^{(l)} = \frac{1}{m} \sum_{j=1}^m \mathbf{v}_{i,j}^{(l)}, \text{ and } \mathbf{C}_i^{(l)} = [\mathbf{v}_{i,1}^{(l)}, \dots, \mathbf{v}_{i,m}^{(l)}] \quad (3)$$

where m is the size of the cluster, l is the level of the cluster in tree, $\mathbf{v}_{i,j}^{(l)}$ is the vector belonging to cluster i at level l such that $\mathbf{v}_j \in \mathbf{C}_i^{(l)}$ and $j = 1, \dots, m$. The key distinction between inner and leaf nodes lies in their contents: Inner nodes store the centroids of their child nodes as values, whereas leaf nodes store the centroids of the actual data clusters as keys and the original vectors as their associated values. We denote the key value pairs as $\mathbf{c}_i^{(l)} \mapsto \mathbf{C}_i^{(l)}$ representing the centroid of the node i and its cluster matrix \mathbf{C}_i containing the vectors at level l . For a B+ANN tree with a height of L , an inner node i at level $L-1$ contains centroids $\mathbf{C}_i^{(L-1)} = [\mathbf{c}_1^{(L)}, \dots, \mathbf{c}_m^{(L)}]$ where each centroid j maps to each cluster at level L , as denoted by $\mathbf{c}_j^{(L)} \mapsto \mathbf{C}_j^{(L)}$. In Phase 2 of Figure 3, the structure of the modified

B+ Tree, which we call B+ANN, is shown with the root node, inner nodes, and leaves that contain the vectors in the vector space.

B+ANN Tree is a self-balancing tree that grows wide by adding clusters based on their centroids to the leaf nodes. For each added cluster to the leaf node, the centroid is added to the inner node that points to the leaf. The inner node and the leaf node update their clusters. Similar to a B+ Tree, it grows horizontally when the nodes are fully loaded (or above some threshold value), and the node splits into two, creating two new centroids that are added to the upper level inner node. The split performs K-Means with 2 clusters, where the centroids of the split nodes are updated. The capacity of the inner node is determined by the κ_{inner} parameter.

Building the B+ANN: In Section 5.1, we obtain multiple clusters with their centroids representing the mean of residing vectors. Instead of adding each vector to the tree one by one, we exploit the hierarchy that was discovered by the previous step in Section 5.1. We traverse the hierarchical structure, as illustrated in Figure 3, and record the number of vectors contained within each visited subtree. If the vector count is lower than the leaf-capacity parameter, κ_{leaf} , then the leaves of the subtree are selected. The selected leaf clusters are highlighted in yellow. Then, we cut the leaf clusters and create the lowest-level nodes of the B+ANN by adding them to the lowest layer as pairs of centroid-clusters. In other words, after the hierarchical Clustering process, we have many pairs of $(c_1, C_1), \dots, (c_m, C_m)$ that we add to the B+ANN Tree, instead of adding each vector one by one to the tree. This way, we accelerate the building process, as well as keep the hierarchical relation between the clusters by respecting the geometry. For each insertion, the centroids are added to the inner (parent) node, starting from the root. Each inner node splits into two if it reaches the inner node capacity denoted by κ_{inner} . The tree grows in balance, resulting in a wide tree with a lower height. Overall, the building algorithm takes two parameters κ_{leaf} and κ_{inner} , and the pairs of centroid-clusters and returns the B+ANN tree.

Once the tree is built, we can save it into to disk, under file named `tree.bin`. We show the storage pattern of the nodes in the Phase-3 of Figure 3 by illustrating the blocks of pages and zooming to a single page structure. Each node is stored in blocks of pages containing the meta data, centroid, and the vectors stored in the node. A key design insight is that the vectors in the same node are stored together such that the vectors are both semantically and physically close. To maximize spatial locality, nodes that are adjacent in the tree are also stored in close proximity on disk. For a sequence of queries that are temporarily close, the proximal similarity in the storage enables frequent access to the same memory locations, consequently, less number of cache misses occur.

Search in the B+ANN: B+ANN retrieves the k -ANNs of a query q by performing Breadth-First Search (BFS) on the tree. As shown in Phase-2 of Figure 3, for a node i in level l , we compute the distances to the lower-level nodes by computing $d(q, c)$, $\forall c \in C_i^{(l)}$. If the selected distance metric is cosine distance, then the computation is vector-matrix multiplication and subtraction (denoted by $1 - q^T C_i^{(l)}$), which can be accelerated by SGEMM operations by using libraries such as cuBLAS, OpenBLAS. Furthermore, in batched queries the operation can further be expedited by matrix-matrix multiplication (e.g., $Q^T C_i^{(l)}$), which speeds up computations significantly using

BLAS or GPU acceleration. This optimization is natural for tree- or cluster-based ANN methods, where you compare a batch of queries to centroids (structured subsets). Graph-based methods (like HNSW, NSG, etc.) typically perform fine-grained, pointer-chasing traversals that are less amenable to matrix-matrix parallelization due to their irregular memory access and dynamic traversal paths.

The traversal is controlled by the priority-queue, which orders the next level nodes based on the distances from their centroids to the queries, prioritizing those with smaller distances by putting them at front. At the next level, we pop nodes from the front of the queue, with the number of nodes controlled by the branching factor parameter β . Each node popped from the queue can be processed in parallel by a thread, and in each thread, we compute the distances to the centroids of the lower nodes and push them to the queue. A lock governs the synchronization of push and pop operations. At the lowest layer, instead of calculating the distance to centroids, we calculate the distance to the data vectors, and return the k -ANNs.

A node, depending on its initialization, can be accessed either memory or disk. For a tree that is fully stored in the disk, when a query comes, we perform Disk I/O for every node and we load the accessed nodes into the memory during traversal. This system maintains a small memory footprint by loading only the traversed nodes to the memory which account for roughly 0.01% of the all nodes in the whole tree. However, continuously allocating new nodes in memory may eventually lead to an out-of-memory (OOM) error. Therefore, we utilize Least Recently Used (LRU) cache policy. The loaded node stays in the memory until it is least recently used. We illustrated this process in Phase 3 of the Figure 3. The control of the LRU queue is run in an independent thread which is synchronized by a lock. The Algorithm 2 shows the pseudo code for searching on B+ANN indexing.

5.3 Building and Traversing the Skip Connections

Tree indexing is the first step in efficiently managing and indexing large volumes of data. To make precise searches, we need finer granularity. As we mentioned earlier, the data can be clustered in the local hubs with thousands of vectors. Therefore, the partitioning at the dense level creates tight regions with a high population of vectors lying within the edges, and querying the nearest object would end up in the wrong region, resulting in suboptimal retrieval, which is known as the *edge problem*. For finer granularity, we introduce *skip-edges* to traverse between neighboring regions and circumvent the edge problem. As shown at Phase-2 of the Figure 3, we are connecting a vector within its leaf node, *inter-connection*, and also a neighbor node, *intra-connection*. The inter-connections represent hops between nodes, whereas the intra-connections enable local searches among a node's nearest vectors whenever a hop is performed. The introduction of skip-edge connections transforms the tree into a graph, yielding a hybrid structure that leverages the complementary advantages of both representations. Next, we describe how skip-connections are specified, how they are created and how we use them in the greedy search.

Building Skip-Edges: The skip-edge connections are governed by two parameters: d_{edge} , which specifies the connection degree determining the number of links established for each vector at the

Algorithm 2 B+ANN Search

```

1: procedure SEARCH( $q, k, \beta, J, d_{\text{edge}}$ )
2:    $outputs \leftarrow []$ ,  $visited \leftarrow []$ 
3:    $Q \leftarrow \text{Queue}(\text{root})$ ,  $PQ \leftarrow \text{PriorityQueue}()$ 
4:   while  $!Q.\text{empty}()$  do
5:     for  $node \in Q.\text{pop\_all}()$  do
6:        $dist \leftarrow \text{dist\_1d\_2d}(node.\text{vectors}, q)$ 
7:        $idx \leftarrow \text{argsort}(dist, k)$ 
8:       if  $node$  is internal then
9:         for  $i \in 1.. \beta$  do
10:           $PQ.\text{push}(node.\text{child}(idx[i]))$ 
11:        end for
12:       else
13:         for  $i \in idx$  do
14:            $v \leftarrow node.\text{vectors}[i]$ 
15:           if  $visited[v.\text{id}] = 0$  then
16:              $outputs.\text{add}(v)$ ,  $visited[v.\text{id}] \leftarrow 1$ 
17:           end if
18:         end for
19:         if  $d_{\text{edge}} > 0$  then
20:           GreedySearch( $q, outputs, k, visited$ )
21:         end if
22:       end if
23:     end for
24:     SyncLRU( $Q$ )
25:      $Q \leftarrow PQ.\text{pop\_top}(\beta)$ 
26:   end while
27:   return  $outputs$ 
28: end procedure
  
```

leaf nodes, and s_{leaf} , which defines the size of the leaf set explored during the connection construction process. Constructing the skip-edge connections requires identifying the nearest leaf nodes for each node. Thereby, we first compute the top- s_{leaf} nearest leaf nodes for every node based on pairwise distances between their centroids. Let N_{leaf} be the total number of leaves, then it requires calculating N_{leaf}^2 pairwise distances of each leaf-node. The number of leaf nodes is determined by the capacity of the leaf nodes, and the expected number of leaves is $N_{\text{leaf}} \approx \lceil N/\kappa_{\text{leaf}} \rceil$, making the total complexity $O(N^2/\kappa_{\text{leaf}}^2)$. If we select $\kappa_{\text{leaf}} = \sqrt{N/\log N}$ then the total complexity reduces to $O(N \log(N))$, for $N = 10^6$ setting $\kappa_{\text{leaf}} = 270$ nodes would be enough to reach this complexity. The computation is accelerated through multi-threading and SGEMM operations, reducing execution time to a few seconds owing to its fully parallelizable nature.

After identifying the top- s_{leaf} closest leaf nodes, intra-connections are established by selecting, for each vector in a leaf node, the top- d_{degree} closest vectors among those contained in the top- s_{leaf} leaves. Each vector in a leaf node connects to its top- d_{degree} closest vectors among the nearest leaves. Compared to HNSW, these connections are shorter decreasing the diameter of the graph and enabling it to reach the closest vector more quickly. Since we calculate distances to each vector among top- s_{leaf} closest leaf nodes, the complexity is $O(\kappa_{\text{leaf}} s_{\text{leaf}} N)$. When we assume $\kappa_{\text{leaf}} = \sqrt{N/\log N}$ and if $s_{\text{leaf}} \leq \sqrt{N \log(N)}$ then overall complexity is strictly less than $O(N^2)$ for building the connections. For $N = 10^6$ setting $s_{\text{leaf}} = 2450$, as we show in our experiments, usually 512 value is enough to reach above 90% recall value.

Algorithm 3 Traversing the Skip-edges

```

1: procedure GREEDYSEARCH( $q, outputs, k, visited$ )
2:    $L \leftarrow outputs$ ,  $L' \leftarrow outputs$ 
3:   for  $v \in outputs$ , where  $visited[v.\text{id}] \leq 1$  do
4:     for  $u \in v.\text{edges}$  where  $visited[u.\text{id}] < 1$  do
5:        $L.\text{add}(u)$ ,  $u.\text{id} \leftarrow 1$ 
6:     end for
7:      $v.\text{id} \leftarrow 2$  ▷ node  $v$  is all discovered
8:   end for
9:    $L \leftarrow \text{get\_nearest\_k}(q, L, k)$  ▷ Retain only  $k$  closest points to  $q$ 
10:  if  $L' \neq L$  then
11:    GreedySearch( $q, L, k, visited$ )
12:  end if
13:  return  $L'$ 
14: end procedure
  
```

Greedy Search: The traversing algorithm, *greedy-search*, is shown in Algorithm 3. We adapt the greedy-search strategy with an important change: We initialize the set of visited vectors, L , with the *outputs* of the tree search, as shown at 20th line in Algorithm 2 and at the 2nd line in Algorithm 3. This allows multiple search seeds to be initialized concurrently during multi-threaded execution, and converge the final set more rapidly by traversing at different branches in parallel, as shown in Figure 10. The visited array is an atomic state variable that can take values 0, 1, or 2, each representing a distinct visitation state: a value of 0 indicates that the vector has not been visited, 1 denotes that it has been visited but its edges have not yet been explored, and 2 signifies that all its edges have been fully discovered. For each vector in the *outputs*, we discover its edges and put them into L . Then we retain the top- k nearest vectors in L . If there is a new vector added to the initial set L , then we recursively call the greedy search again. If there are no changes in the output vectors, then we stop traversing and return the final L .

Usage of Skip-Edges: During the indexing of a dataset \mathcal{D} , skip-edge connections are not constructed by default; instead, the user may optionally enable their creation through a configuration parameter. The created graph structure is maintained in memory, yet it can also be serialized to the disk for persistence. Compared to the tree, skip-edges incur a higher computational cost to build, we expose this option as a user-defined argument to enable finer-grained search when required. In the following section, we utilized this feature to first index extreme datasets ($|\mathcal{D}| \gg$ billions) by tree indexing and creating view representations with skip-edge connections.

5.4 View Creation and B+ANN Usage

As we defined in Section 4, for a query q_t at time t we extract the view from the B+ANN Tree by $V(q_t, \mathcal{T}, k) = \mathcal{T}'$ and obtain the graph created $G' = (\mathcal{L}(\mathcal{T}'), \mathcal{E})$ by connecting the leaves of subtree $\mathcal{L}(\mathcal{T}')$ with the skip-edge connections, where \mathcal{E} represents the edges between pairs of vectors. Then, the subsequent queries q_{t+1}, q_{t+2}, \dots are served this representation using B+ANN search (Algorithm 2). If the retrieved k -ANN vectors of any of the subsequent queries do not exist in the true k -NNs, i.e., recall hits to zero, we extract another view. We call the duration between two succeeding views as the *view survival time*. As shown in Figure 2b,

when the queries are temporarily correlated, the survival time of a view can last up to 1000 queries. Moreover, the duration can be increased by setting the k parameter of the view function to a high value (e.g., 1000) to populate a view that lasts longer.

The extraction of a view can be applied to a B+ANN tree \mathcal{T} residing either in memory or on disk. Since the operation relies on efficient tree-based search, retrieving k -ANNs ($k < 1000$) is extremely fast, and constructing a view with skip-edge connections for $N < 1000$ nodes typically completes within seconds. The value 1000 here denotes an arbitrarily large constant. Most importantly, when \mathcal{T} resides in the disk, it can asynchronously be updated by inserting new vectors, while the extracted view \mathcal{T}' responds to the incoming queries. Separating the computation to disk and memory allows us to store a clean, lightweight data structure on disk with locality-improved storage that allows fewer cache misses, and we move the fine-grained computation to the memory. Therefore, we can store a gigantic amount of data in a disk without any spurious and complex components, such as edges in a graph indexing.

Another important aspect of view creation is its semantic representation. It represents a collection of semantically related information of a query vector, and when this query is related to a particular topic, the view encapsulates the most relevant information of that topic. This opens the door for various applications. In terms of access control, a user can have access to a particular view of data that represents a subset of the information through a specific query. Moreover, it is possible to extract multiple views from a dataset and use the information provided by them as an expertise in different topics. Therefore, the area confined by the view makes it possible to search for the ranges of particular interest, which is useful for especially dissimilar queries. Once a view is extracted for a query, we define a context, and we can find the most dissimilar queries within that context. For example, if we are finding the most dissimilar "cereal" of a given cereal item, in ordinary VDBs, we would retrieve highly unrelated items. On the other hand, by the view creation of the cereal item, we determined the border of our search with a context and can retrieve the most dissimilar "cereal" for the given item. Next, we evaluate the performance of B+ANN.

6 EVALUATION

6.1 Datasets and Experimental Setup

In our experiments, we have used two benchmark datasets: The first is Glove-1.2M containing 1.2 million 100- and 200-dimensional word embeddings introduced by [48]. We indexed the vectors in this dataset based on the cosine distance and calculate the recall value of the same test split of [6]. To observe the scalability and the performance of Euclidian Distance, we utilized SIFT-1B dataset from [1] containing 1 billion 128-dimensions of image descriptors. Furthermore, to run low scale experiments such as dissimilarity search, we used the Spotify dataset [51] containing 243k vectors with 256 dimensions.

We compare two Instruction Set Architectures, Arm64 and x86. For Arm64, we used an Apple M4 Max system with 16 Performance cores and 32 GB of unified memory, running without virtualization. For the x86 architecture, we employed a workstation virtualization with Intel Xeon Platinum CPUs featuring 128 cores and 64 GB

of memory, where we also measured the utilization of L1 and L2 caches.

For implementation, we used C++17 for our codebase and the CBLAS library to perform SIMD operations to calculate distance metrics. As an evaluation metric, we followed standard benchmark set-up from [6] and observed speed-recall trade-off by measuring 10-Recall (%) and Query Per Second (QPS) (1/s) performance.

6.2 In-Memory Performance of B+ANN

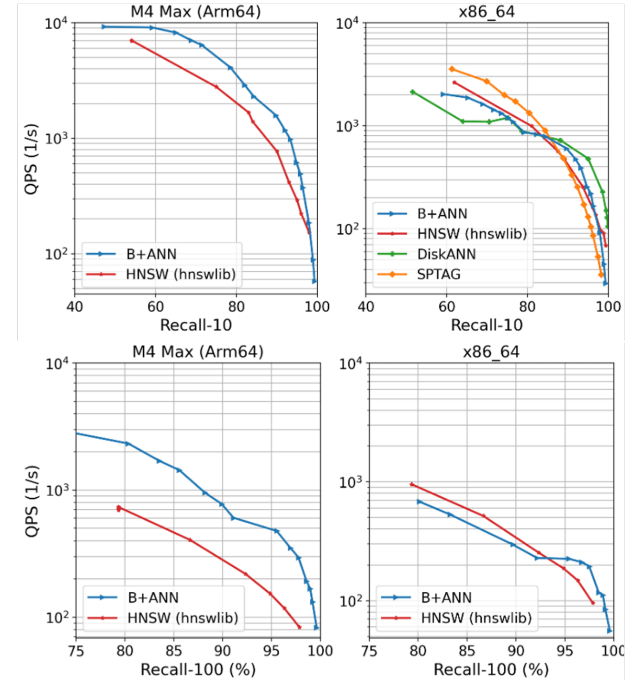


Figure 4: In-memory performance of ANN algorithms and B+ANN. We show QPS vs Recall-10 and Recall-100 curves of benchmark algorithms and B+ANN for Arm64 and x86 architectures.

Based on this setup, we measured the performance of B+ANN and multiple benchmark algorithms. We selected HNSW as the main graph-based algorithm to observe the performance change by our design based on our motivation in section 3. We enriched the comparison with the two SOTA disk-based ANN algorithms, DiskANN [30], and SPTAG [13]. While DiskANN is built on a sparse neighborhood graph, SPTAG is also a hybrid approach that utilizes space partition and multiple Relative Neighbourhood Graphs. Our HNSW experiments were conducted with `hnslib` [37], a C++ implementation. While `hnslib` and B+ANN are architecture-agnostic, DiskANN and SPTAG are tied to architecture-specific features, and they require containerization to be implemented in other architectures. All the baseline methods can perform SIMD accelerations and utilize multi-threading.

In this section, we compared the in-memory performance of the used SOTA algorithms with B+ANN. Therefore, we build the

Architecture Type x86_64				
Method	IPC (1/s)	L1 Load Miss (%) ↓	Branch Miss (%) ↓	QPS (1/s) ↑
HNSW	0.68	19.76	3.19	186.64
B+ANN	0.29	15.96	3.21	225.19
Rel. Gain	-	-19.23%	+0.62%	+20.65%

Table 2: We measure multiple performance statistics in x86 and s390x for HNSW and B+ANN at the 95% 10-Recall value.

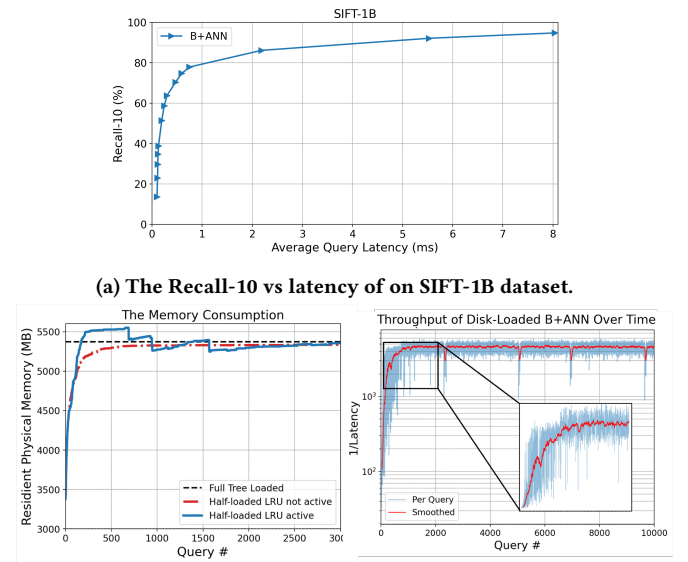
Hierarchically Clustered B+Tree in memory and create the skip-edge connections between nodes. We make an analysis of the disk performance in section 6.3. Following [30] parameter selection, for all the algorithms, during construction, we set the edge degree to $M = 128$, and the effective search parameter to $ef_C = 512$. For the architecture-specific parameters, e.g., Vamana indices R, L , and penalty constant α , we use the default parameters listed on their corresponding repositories. Accordingly, we set the parameters of B+ANN as follows: $\kappa_{leaf} = 2048$, $\kappa_{inner} = 1024$, $d_{edge} = 128$, and $s_{leaf} = 512$, and built the tree and created the skip-connections all in memory. Figure 6 shows the graph built time for all the algorithms in different architectures. We report the time it takes to build the tree and skip-edges. The result shows that B+ANN has the fastest build time in arm64 and s390x architectures, while having the third fastest build time in x86. SPTAG, on the other hand, took more than 3 times the build time of B+ANN.

After the indexing, we perform search multiple times by changing the search width parameter, e.g. ef of algorithms ranging from 5 to 1200 and measure the recall values. The corresponding parameter in B+ANN is the branching factor, β , which ranges from 5 to 100. Lastly, all algorithms were executed using the same number of threads, $threads = 10$. We also performed experiments keeping the thread count to 1, however, B+ANN outperforms the other algorithms with a larger gap when $threads > 1$ showing the importance of cache and memory locality.

Figure 4 shows the speed-recall curves of the algorithms obtained using the described parameters and experimental setup. Compared to HNSW, B+ANN achieves a 10× speedup at 10-Recall and a 50× speedup at 100-Recall in arm64 architecture and 1.1× to 2× speed up in x86, while showing the same recall high value. Relative to DiskANN and SPTAG, B+ANN shows comparable performance yet these algorithms require CPU specific speed-ups e.g. AVX512. Next, we show that B+ANN is much more advantageous for disk implementation.

6.3 On-Disk Performance and Memory Usage

For the on-disk experiments, we utilized the SIFT-1B dataset and built the B+ANN tree on the disk, which took 2 hours with 150GB maximum memory usage. This is 24× faster compared to DiskANN built time and 350GB less memory usage[30]. The reason is that B+ANN tree building time has the complexity of $O(n \log n)$. The search performance is shown in Figure 5a. The plot shows that B+ANN can reach 99.8% Recall-10 in less than 9ms and 80.0% recall in less than 1ms. The results show that B+ANN can respond to queries within milliseconds with high precision, even for huge datasets without requiring full in-memory indexing, thereby drastically reducing hardware cost and memory footprint. This capability



(a) The Recall-10 vs latency of on SIFT-1B dataset.
(b) The left shows how LRU balances the memory consumption when a half-loaded (half of the nodes are in memory and the other half is on disk) tree is used. The right shows how B+ANN balances the throughput as it performs search by loading nodes from disk to memory (it starts with zero-loaded tree).

Figure 5: B+ANN Performance for the SIFT-1B dataset

is critical in applications such as large-scale recommendation engines, semantic search systems, and knowledge retrieval platforms, where responsiveness and accuracy jointly determine user satisfaction and system scalability.

Figure 5b shows our second analysis of disk-based search in B+ANN. During the search, B+ANN uses hybrid memory usage by loading the leaf-nodes from disk to memory. Initially, all the nodes are located on disk, and the memory capping is active. As we perform the vector search by traversing the levels of the tree, B+ANN loads the nodes to memory through LRU. For example, the Figure 5b shows the memory consumption and throughput as we perform searches on a B+ANN index tree with half of the nodes located on disk and the other half located in memory. We make two observations: (i) The LRU queue balances the memory usage when the memory exceeds the threshold, and it asynchronously dumps the least recently used nodes into the disk. A natural question is, why can't we let this process be handled by the OS and its swapping mechanism, especially in macOS, since everything operates on the same memory fabric? The reason is that when the OS swaps inactive memory, the paging and addressing are handled by the OS with respect to its own grouping methods; however, B+ANN has a structured storage system that already maximizes the locality. It keeps semantically close vectors (and nodes) also physically close on disk, thereby increasing locality and faster I/O operations. (ii) We observe that as the searching continues, the throughput exhibits asymptotic growth. Initially, the number of I/O operations is high due to the tree being fully located inside the disk. As we index queries, we load nodes from disk to memory, and the probability

of nodes we fetch from the memory (LRU queue) increases; consequently, the latency decreases. The results exemplify the robust convergence property of the B+ANN, attaining a steady operating point, ensuring long-term predictability and stability.

6.4 Average Hops Comparison

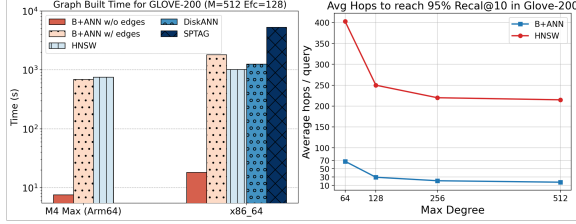


Figure 6: Figure on left shows the graph build time comparison of each algorithm for different architectures. The plot on right shows the average-hop comparison between B+ANN and HNSW (lower is better).

The plot on the left in Figure 6 shows the graph-building time of baseline indexing algorithms and B+ANN. We report the total time taken for B+ANN to build the Hierarchical Clustering B+Tree and the skip-edge connections. Also, we calculated that it takes 84.3% of total indexing time to build skip-edge connections. The difference is because the complexity of building the tree is $O(n \log(n))$ lower than creating the skip-edge connections, $O(n_{leaf} \cdot n \cdot d_{edge})$. However, the complexity of building the skip-edge connections can be reduced by adding the vectors to the leaf-nodes in an ordered way, e.g., based on their distance to their centroid. Connecting vectors to the closest vector in the neighboring node, therefore, would require less computation. Based on the scope of our paper, we leave it as future work.

To test the diameter of skip-edge connections, we compare the number of visited nodes in an HNSW graph with the number of visited nodes in B+ANN with skip-edge connections. The Figure 6 shows the average hop comparison between HNSW and B+ANN to reach Recall-10 using set of degrees $d_{edge} = \{64, 128, 256, 512\}$ building B+ANN and corresponding M parameter for HNSW. Then we increased the effective search parameter, ef , for HNSW and branching factor, β , for B+ANN until we observed an average 95% Recall value. The plot shows that B+ANN uses 15× fewer hops than HNSW. Based on this observation, B+ANN creates shorter connections, thereby decreasing the diameter and enabling it to reach the closest vector more quickly. Fewer hops also decreases the number of I/O, which is critical during hybrid memory search and when memory capping is active.

6.5 Exploiting Temporal Correlation by B+ANN

One of the biggest advantages of B+ANN appears when the input queries are temporally correlated. To simulate this, we have sorted the incoming queries based on their distances to each other. For a query at time t denoted by q_t , the next query is within proximity yet it has not appeared before, represented as $q_{t+1} \in R(q_t)$ and $R \subset S \setminus Q_{\text{prev}}$, where $R(q_t)$ is the vectors at proximity of q_t computed on the unused queries and $Q_{\text{prev}} = \{q_1, \dots, q_{t-1}\}$ is the set of previous

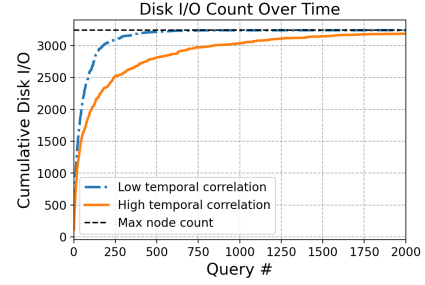


Figure 7: Plot shows the cumulative number of Disk I/O operations performed when there is a high temporal and low temporal correlation in SIFT-1B dataset.

queries before time t . The Figure 7 shows the total Disk I/O count as the number of queries with high temporal correlation compared to random order. In randomly selected queries, the graph is discovered more quickly by visiting the unvisited nodes more frequently. In contrast, high temporal correlation shows a slower increase in Disk I/O count compared to the random selection. The answer to the next query can be retrieved from the node that was already put in memory in the earlier responses. The critical impact of this property is also observed in Figure 2a, the survival time of the view can reach up to 1000 queries due to responding from the created view in memory, and the incoming query will be in the view. Therefore, if temporal correlation exists, B+ANN will eventually delay the new view creation and reduce the average response time.

6.6 Balanced Growth and Insertion

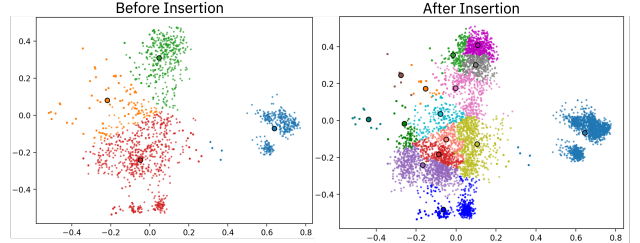


Figure 8: Visualization of the clustering after insertion: initial cluster mapping is updated as new vectors are added (e.g., the before-insertion green cluster gets split into 4 different clusters).

For an indexing algorithm, being flexible and updatable is essential, especially in systems that terabytes of fresh data continuously coming. One of the reasons of selecting B+ Tree architecture is this flexibility and being able to grow in width without performance depreciation. In B+ANN, the incoming vector is inserted to one of the leaf nodes and the leaf is split if it reaches the capacity. This split operation performed using K-Means, and the vectors inside that leaf node are divided into two clusters creating two new centroids that needs to be added into inner nodes. The number of vectors that needs to be inserted for a node to split increases exponentially as we

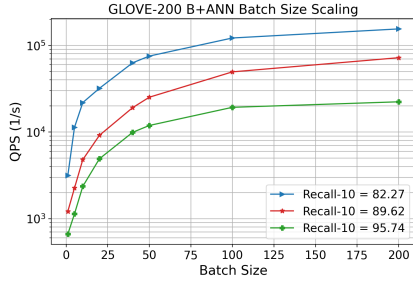


Figure 9: Scalability of query throughput (QPS) with respect to batch size, in GLOVE-200. Larger batch sizes generally improve throughput until saturation is reached.

go from lower levels to higher levels. Hence, for an input vector, the update mechanism locally adjusts branches without drastic update on overall tree index structure. Figure 8 illustrates the growth in the B+ANN. We performed PCA on the vectors that are indexed to visualize in two-dimensional space and observe the clusters that are created and assigned. On left, only 15% of the data is indexed which has 4 leaf nodes. On right, rest of the data is inserted and the growth on the clusters are shown. Observe that the clusters are separated w.r.t. their previous location, e.g., the green cluster on left is subdivided into 4 clusters respecting the distances. Secondly, observe the blue cluster on the right side of Before-Insertion and After-Insertion plots. Vectors in the vicinity of the blue cluster are assigned to that cluster, and the corresponding node is updated without a split operation since its capacity is not reached.

6.7 Impact of Batch Size on Performance

The Figure 9 plots the relation between QPS and batch size and testing the scalability of B+ANN as the workload gradually increased. The colored lines indicate configurations with a constant Recall-10 value, while the batch size is varied and all other parameters are held fixed. Here, we calculated $QPS = \frac{N_{queries}}{T_{total}}$. When queries are batched, vector-matrix operations are replaced by matrix-matrix operations during tree traversal, which is shown in Figure 10. Consequently, the scalability of tree traversal depends on CBLAS SGEMM efficiency, which exhibits exponential growth. In contrast, during skip-edge traversal, each query vector in the batch is processed by an individual thread, limiting scalability to the available number of threads. Therefore, all the lines in Figure 9 shows asymptotic growth with rapid increase initially and attain a steady QPS thereafter. Moreover, we observe up to $\times 100$ increase in QPS as we increase the batch size.

6.8 Evaluating Dissimilarity Search

Unlike the traditional similarity queries, dissimilarity queries are used to identify semantically different entities. For example, in Db2 SQL Data Insights, dissimilarity queries are often used to extract outliers [28].

To measure the performance of the dissimilarity search functionality of B+ANN, we reversed the problem by a labeled dataset where each vector has a label set that contains the IDs of the top-k farthest vectors. Using this setup, we query the B+ANN using the

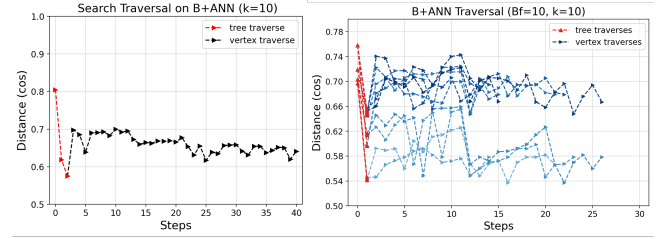


Figure 10: We show the B+ANN traversal for a query and a batched query

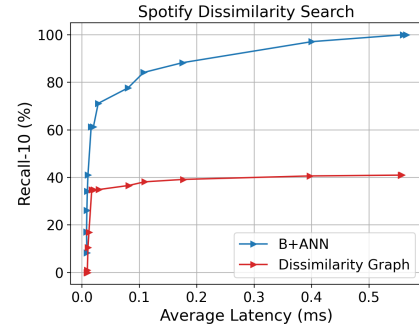


Figure 11: We evaluate the dissimilarity performance of B+ANN relative to a baseline dissimilarity graph (higher is better).

dissimilarity flag and measure the Recall-10. Then, we developed a new baseline algorithm, as dissimilarity-based vector search has been sparsely studied in the literature, and current HNSW-type graph algorithms cannot support dissimilarity queries. We created a Relative Neighborhood-graph (RNG) based on the distance between vectors, and we connect two vectors if they are farther from each other than any other vectors. The performance of this baseline and B+ANN is shown in Figure 11. B+ANN can reach 100% Recall within less than 0.6ms, while dissimilarity-RNG can reach up to 40%. We observe that dissimilarity-RNG oscillates between the same graph nodes, therefore converges to a local solution.

7 CONCLUSION

This paper presents B+ANN, a novel disk-based ANN algorithm, that improves functionality, result accuracy, and performance over HNSW, currently the most used ANN algorithm in Vector Databases. Our extensive performance evaluation using a variety of large vector datasets demonstrates that B+ANN improves in-memory and disk access patterns leading to improved spatial and temporal locality, leading to improved computation acceleration opportunities. The B+ANN tree approach also enables efficient execution of dissimilarity queries, which are not supported by HSNW-based indices. As a future work, we want to further explore the notion of semantic views and its impact on the index architecture. We also want to explore opportunities for memory reduction using low-precision floating point representations.

REFERENCES

[1] Laurent Amsaleg and Hervé Jégou. 2010. Datasets for approximate nearest neighbor search. <http://corpus-texmex.irisa.fr/>. [Online; accessed 10-July-2024].

[2] Yuwei An, Yihua Cheng, Seo Jin Park, and Junchen Jiang. 2025. Hyperrag: Enhancing quality-efficiency tradeoffs in retrieval-augmented generation with reranker kv-cache reuse. *arXiv preprint arXiv:2504.02921* (2025).

[3] Alexandr Andoni and Piotr Indyk. 2008. Near-optimal hashing algorithms for approximate nearest neighbor in high dimensions. *Commun. ACM* 51, 1 (2008), 117–122.

[4] Alexandr Andoni, Piotr Indyk, Thijs Laarhoven, Ilya Razenshteyn, and Ludwig Schmidt. 2015. Practical and optimal LSH for angular distance. *Advances in neural information processing systems* 28 (2015).

[5] David Arthur and Sergei Vassilvitskii. 2006. *k-means++: The advantages of careful seeding*. Technical Report. Stanford.

[6] Martin Aumüller, Erik Bernhardsson, and Alexander Faithfull. 2018. ANN-Benchmarks: A Benchmarking Tool for Approximate Nearest Neighbor Algorithms. *arXiv:1807.05614* [cs.IR] <https://arxiv.org/abs/1807.05614>

[7] Artem Babenko and Victor Lempitsky. 2015. The Inverted Multi-Index. *IEEE Transactions on Pattern Analysis and Machine Intelligence* 37, 6 (2015), 1247–1260. <https://doi.org/10.1109/TPAMI.2014.2361319>

[8] Dmitry Baranukh, Artem Babenko, and Yury Malkov. 2018. Revisiting the inverted indices for billion-scale approximate nearest neighbors. In *Proceedings of the European Conference on Computer Vision (ECCV)*. 202–216.

[9] Rajesh Bordawekar and Oded Shmueli. 2016. Enabling Cognitive Intelligence Queries in Relational Databases using Low-dimensional Word Embeddings. *CoRR* abs/1603.07185 (2016). <http://arxiv.org/abs/1603.07185>

[10] Rajesh Bordawekar and Oded Shmueli. 2017. Using Word Embedding to Enable Semantic Queries in Relational Databases. In *Proceedings of the 1st Workshop on Data Management for End-to-End Machine Learning* (Chicago, IL, USA) (DEEM’17). ACM, New York, NY, USA, Article 5, 4 pages. <https://doi.org/10.1145/3076246.3076251>

[11] Moses S. Charikar. 2002. Similarity Estimation Techniques from Rounding Algorithms. In *Proceedings of the Thiry-fourth Annual ACM Symposium on Theory of Computing*. 380–388.

[12] Jianly Chen, Shitao Xiao, Peitian Zhang, Kun Luo, Defu Lian, and Zheng Liu. 2024. Bge m3-embedding: Multi-lingual, multi-functionality, multi-granularity text embeddings through self-knowledge distillation. *arXiv preprint arXiv:2402.03216* (2024).

[13] Qi Chen, Haidong Wang, Mingqin Li, Gang Ren, Scarlett Li, Jeffery Zhu, Jason Li, Chuanjie Liu, Lintao Zhang, and Jingdong Wang. 2018. SPTAG: A library for fast approximate nearest neighbor search. <https://github.com/Microsoft/SPTAG>

[14] Qi Chen, Bing Zhao, Haidong Wang, Mingqin Li, Chuanjie Liu, Zengzhong Li, Mao Yang, and Jingdong Wang. 2021. Spann: Highly-efficient billion-scale approximate nearest neighborhood search. *Advances in Neural Information Processing Systems* 34 (2021), 5199–5212.

[15] Chroma. 2022. Chroma. <https://github.com/chroma-core/chroma>.

[16] Paolo Ciaccia, Marco Patella, Pavel Zezula, et al. 1997. M-tree: An efficient access method for similarity search in metric spaces. In *Vldb*, Vol. 97. Citeseer, 426–435.

[17] Mayur Datar, Nicole Immorlica, Piotr Indyk, and Vahab S Mirrokni. 2004. Locality-sensitive hashing scheme based on p-stable distributions. In *Proceedings of the twentieth annual symposium on Computational geometry*. 253–262.

[18] Matthijs Douze, Alexandr Guzhva, Chengqi Deng, Jeff Johnson, Gergely Szilvassy, Pierre-Emmanuel Mazaré, Marin Lomeli, Lucas Hosseini, and Hervé Jégou. 2024. The Faiss library. (2024). *arXiv:2401.08281* [cs.LG]

[19] Elasticsearch. 2015. Elasticsearch. <https://www.elastic.co/>.

[20] Jerome H Friedman, Jon Louis Bentley, and Raphael Ari Finkel. 1977. An algorithm for finding best matches in logarithmic expected time. *ACM Transactions on Mathematical Software (TOMS)* 3, 3 (1977), 209–226.

[21] Luyu Gao and Jamie Callan. 2022. Long Document Re-ranking with Modular Re-ranker. In *Proceedings of the 45th International ACM SIGIR Conference on Research and Development in Information Retrieval* (Madrid, Spain) (SIGIR’22). Association for Computing Machinery, New York, NY, USA, 2371–2376. <https://doi.org/10.1145/3477495.3531860>

[22] Siddharth Gollapudi, Neel Karia, Varun Sivashankar, Ravishankar Krishnaswamy, Nikit Begwani, Swapnil Raz, Yiyong Lin, Yin Zhang, Neelam Mahapatro, Premkumar Srinivasan, et al. 2023. Filtered-diskann: Graph algorithms for approximate nearest neighbor search with filters. In *Proceedings of the ACM Web Conference 2023*. 3406–3416.

[23] Zengyang Gong, Yuxiang Zeng, and Lei Chen. 2025. Accelerating Approximate Nearest Neighbor Search in Hierarchical Graphs: Efficient Level Navigation with Shortcuts. *Proceedings of the VLDB Endowment* 18, 10 (2025).

[24] Ruiqi Guo, Philip Sun, Erik Lindgren, Quan Geng, David Simcha, Felix Chern, and Sanjiv Kumar. 2020. Accelerating large-scale inference with anisotropic vector quantization. In *International Conference on Machine Learning*. PMLR, 3887–3896.

[25] Antonin Guttman. 1984. R-trees: A dynamic index structure for spatial searching. In *Proceedings of the 1984 ACM SIGMOD international conference on Management* of data. 47–57.

[26] Yikun Han, Chunjiang Liu, and Pengfei Wang. 2023. A comprehensive survey on vector database: Storage and retrieval technique, challenge. *arXiv preprint arXiv:2310.11703* (2023).

[27] IBM Corp. 2025. Db2 for Linux, UNIX and Windows Vector values 12.1.x. <https://www.ibm.com/docs/en/db2/12.1.x?topic=list-vector-values>

[28] IBM Corp. 2025. Running AI Queries with SQL Data Insights. <https://www.ibm.com/docs/en/db2-for-zos/13.0.0?topic=running-ai-queries-sql-data-insights>

[29] Omid Jafari, Preeti Maurya, Parth Nagarkar, Khandker Mushfiqul Islam, and Chidambaram Crushev. 2021. A survey on locality sensitive hashing algorithms and their applications. *arXiv preprint arXiv:2102.08942* (2021).

[30] Suhas Jayaram Subramanyam, Fnu Devvrit, Harsha Vardhan Simhadri, Ravishankar Krishnamamy, and Rohan Kadekodi. 2019. Diskann: Fast accurate billion-point nearest neighbor search on a single node. *Advances in neural information processing Systems* 32 (2019).

[31] Hervé Jégou, Romain Tavenard, Matthijs Douze, and Laurent Amsaleg. 2011. Searching in one billion vectors: re-rank with source coding. *CoRR* abs/1102.3828 (2011). *arXiv:1102.3828* <http://arxiv.org/abs/1102.3828>

[32] Jeff Johnson, Matthijs Douze, and Hervé Jégou. 2019. Billion-scale similarity search with GPUs. *IEEE Transactions on Big Data* 7, 3 (2019), 535–547.

[33] Hervé Jégou, Matthijs Douze, and Cordelia Schmid. 2011. Product Quantization for Nearest Neighbor Search. *IEEE Transactions on Pattern Analysis and Machine Intelligence* 33, 1 (2011), 117–128. <https://doi.org/10.1109/TPAMI.2010.57>

[34] Yannis Kalantidis and Yannis Avrithis. 2014. Locally optimized product quantization for approximate nearest neighbor search. In *Proceedings of the IEEE conference on computer vision and pattern recognition*. 2321–2328.

[35] Yannis Katsis, Sara Rosenthal, Kshitij Fadnis, Chulaka Gunasekara, Young-Suk Lee, Lucian Popa, Vraj Shah, Huaiyu Zhu, Danish Contractor, and Marina Danilevsky. 2025. Mtrag: A multi-turn conversational benchmark for evaluating retrieval-augmented generation systems. *Transactions of the Association for Computational Linguistics* 13 (2025), 784–808.

[36] Patrick Lewis, Ethan Perez, Aleksandra Piktus, Fabio Petroni, Vladimir Karpukhin, Naman Goyal, Heinrich Kötter, Mike Lewis, Wen-tau Yih, Tim Rocktäschel, et al. 2020. Retrieval-augmented generation for knowledge-intensive nlp tasks. *Advances in Neural Information Processing Systems* 33 (2020), 9459–9474.

[37] Yury Malkov et al. [n.d.]. *hnslib: Hierarchical Navigable Small World graphs*. <https://github.com/nmslib/hnslib> [Online; accessed 28-September-2025].

[38] Yury Malkov, Alexander Ponomarenko, Andrey Logvinov, and Vladimir Krylov. 2014. Approximate nearest neighbor algorithm based on navigable small world graphs. *Information Systems* 45 (2014), 61–68.

[39] Yu A Malkov and Dmitry A Yashunin. 2018. Efficient and robust approximate nearest neighbor search using hierarchical navigable small world graphs. *IEEE transactions on pattern analysis and machine intelligence* 42, 4 (2018), 824–836.

[40] Magdalena Dobson Manohar, Zheqi Shen, Guy Blelloch, Laxman Dhulipala, Yan Gu, Harsha Vardhan Simhadri, and Yihan Sun. 2024. ParlayANN: Scalable and Deterministic Parallel Graph-Based Approximate Nearest Neighbor Search Algorithms. In *Proceedings of the 29th ACM SIGPLAN Annual Symposium on Principles and Practice of Parallel Programming*. 270–285.

[41] Tomas Mikolov, Kai Chen, Greg Corrado, and Jeffrey Dean. 2013. Efficient Estimation of Word Representations in Vector Space. *CoRR* abs/1301.3781 (2013). <http://arxiv.org/abs/1301.3781>

[42] Marius Muja and David G Lowe. 2014. Scalable nearest neighbor algorithms for high dimensional data. *IEEE transactions on pattern analysis and machine intelligence* 36, 11 (2014), 2227–2240.

[43] Javier Vargas Munoz, Marcos A Gonçalves, Zanoni Dias, and Ricardo da S Torres. 2019. Hierarchical clustering-based graphs for large scale approximate nearest neighbor search. *Pattern Recognition* 96 (2019), 106970.

[44] Nvidia Inc. 2024. cuVS: Vector Search and Clustering on the GPU. <https://github.com/rapidsai/cuvs>

[45] Hiroyuki Ootomo, Akira Naruse, Corey Nolet, Ray Wang, Tamas Feher, and Yong Wang. 2023. Cagra: Highly parallel graph construction and approximate nearest neighbor search for gpus. *arXiv preprint arXiv:2308.15136* (2023).

[46] Oracle Inc. 2025. Oracle AI Database 26i. <https://www.oracle.com/database/ai-native-database-26ai>

[47] James Jie Pan, Jianguo Wang, and Guoliang Li. 2023. Survey of vector database management systems. *arXiv preprint arXiv:2310.14021* (2023).

[48] Jeffrey Pennington, Richard Socher, and Christopher D Manning. 2014. Glove: Global vectors for word representation. In *Proceedings of the 2014 conference on empirical methods in natural language processing (EMNLP)*. 1532–1543.

[49] Jie Ren, Minjia Zhang, and Dong Li. 2020. Hm-ann: Efficient billion-point nearest neighbor search on heterogeneous memory. *Advances in Neural Information Processing Systems* 33 (2020), 10672–10684.

[50] Joobo Shim, Jaewon Oh, HongChan Roh, Jaeyoung Do, and Sang-Won Lee. 2025. Turbocharging Vector Databases using Modern SSDs. *Proceedings of the VLDB Endowment* 18, 11 (2025).

[51] Spotify. 2017. ANNOY. <https://github.com/spotify/annoy>.

[52] Philip Sun, David Simcha, Dave Dopson, Ruiqi Guo, and Sanjiv Kumar. 2024. SOAR: improved indexing for approximate nearest neighbor search. *Advances in*

Neural Information Processing Systems 36 (2024).

[53] Ashish Vaswani, Noam Shazeer, Niki Parmar, Jakob Uszkoreit, Llion Jones, Aidan N. Gomez, Łukasz Kaiser, and Illia Polosukhin. 2023. Attention Is All You Need. arXiv:1706.03762 [cs.CL] <https://arxiv.org/abs/1706.03762>

[54] Jianguo Wang, Xiaomeng Yi, Rentong Guo, Hai Jin, Peng Xu, Shengjun Li, Xiangyu Wang, Xiangzhou Guo, Chengming Li, Xiaohai Xu, et al. 2021. Milvus: A purpose-built vector data management system. In *Proceedings of the 2021 International Conference on Management of Data*. 2614–2627.

[55] Jingdong Wang and Ting Zhang. 2018. Composite quantization. *IEEE transactions on pattern analysis and machine intelligence* 41, 6 (2018), 1308–1322.

[56] Jingdong Wang, Ting Zhang, Jingkuan Song, Nicu Sebe, and Heng Tao Shen. 2016. A Survey on Learning to Hash. *CoRR* abs/1606.00185 (2016). arXiv:1606.00185 <http://arxiv.org/abs/1606.00185>

[57] Wen Yang, Tao Li, Gai Fang, and Hong Wei. 2020. Pase: Postgresql ultra-high-dimensional approximate nearest neighbor search extension. In *Proceedings of the 2020 ACM SIGMOD international conference on management of data*. 2241–2253.

[58] Ziyang Yue, Bolong Zheng, Ling Xu, Kanru Xu, Shuhao Zhang, Yajuan Du, Yunjun Gao, Xiaofang Zhou, and Christian Jensen. 2025. Select Edges Wisely: Monotonic Path Aware Graph Layout Optimization for Disk-based ANN Search. *Proceedings of the VLDB Endowment* 18, 11 (2025).

[59] Qianxi Zhang, Shuotao Xu, Qi Chen, Guoxin Sui, Jiadong Xie, Zhizhen Cai, Yaoqi Chen, Yinxuan He, Yuqing Yang, Fan Yang, et al. 2023. {VBASE}: Unifying Online Vector Similarity Search and Relational Queries via Relaxed Monotonicity. In *17th USENIX Symposium on Operating Systems Design and Implementation (OSDI 23)*. 377–395.

[60] Weijie Zhao, Shulong Tan, and Ping Li. 2020. Song: Approximate nearest neighbor search on gpu. In *2020 IEEE 36th International Conference on Data Engineering (ICDE)*. IEEE, 1033–1044.